Synthesis of Molecular Brushes with Gradient in Grafting Density by Atom Transfer Polymerization

Hans G. Börner,[†] David Duran,[†] Krzysztof Matyjaszewski,*[,†] Marcelo da Silva,[†] and Sergei S. Sheiko*[,‡]

Center for Macromolecular Engineering, Department of Chemistry, Carnegie Mellon University, 4400 Fifth Ave., Pittsburgh, Pennsylvania 15213, and Department of Chemistry, University of North Carolina at Chapel Hill, Chapel Hill, North Carolina 27599

Received December 3, 2001; Revised Manuscript Received February 19, 2002

ABSTRACT: Macromolecular brushes with a gradient of side-chain spacing along the backbone have been synthesized by the "grafting from" approach using atom transfer radical polymerization. A macroinitiator was prepared in two steps, first by conducting a gradient copolymerization of MMA and HEMA-TMS followed by transformation of the resulting poly(MMA-*grad*-HEMA-TMS) to poly(MMA-*grad*-BPEM). The gradient composition of the macroinitiator was a forced gradient formed by continuous feeding of HEMA-TMS during MMA polymerization. The gradient structure was characterized by monitoring monomer conversion (GC) and molecular weight evolution (GPC) during copolymerization. AFM measurements demonstrated the characteristic anisotropy of the molecular structure by resolving individual brush molecules with a bulky head and a thin tail.

Introduction

Comblike polymers with long side chains attached to a flexible backbone give functional macromolecules with cylindrical shape, variable length, and the directed motion capability.[1] In contrast to typical graft copolymers, which are loosely grafted, the characteristic feature of brush molecules is high grafting density, recurrently one graft per backbone repeat unit.[2] The dense spacing of the side chains results in steric repulsion that induces an increase of the persistent length as well as the contour length of the polymer backbone. Both synthesis and analysis of these systems are challenging. Progress in this field would lead to better understanding of structural control to design synthetic polymer molecules as components in nanomechanical devices.[1] One of the prerequisites of directed action produced by such molecular cylinders would be their broken symmetry, e.g., anisotropy of the chemical structure along the backbone. In this paper we report on preparation of molecular brushes with gradient of grafting density.

Three synthetic routes to macromolecular brushes, which also have been applied to loosely grafted systems, are described in the literature: (i) "grafting onto" (attachment of side chains to the backbone),[3−6] (ii) "grafting through" (homopolymerization of macromonomers),[2,7−12] and (iii) "grafting from" (grafting side chains from the backbone).[13−15] These methods can be combined with controlled polymerization techniques which enable independent control of the molecular parameters i.e., degree of polymerization and polydispersity of main and side chain polymers, overall grafting density, and grafting uniformity. So far, variation of the latter parameter has not been studied in the synthesis of macromolecular brushes (Scheme 1).

The controlled synthesis of macromolecular brushes by "grafting from" a macroinitiator via copper-mediated atom transfer polymerization (ATRP)[16−20] was described previously.[13−15,21,22] The macroinitiator bearing ATRP initiating groups as side groups in each repeating unit was obtained by ATRP of 2-(trimethylsilyloxy)ethyl

Scheme 1. Subsequent Synthesis of the Macroinitiator Precursor (I), the Macroinitiator (II), and Macromolecular Brush Copolymer (III)

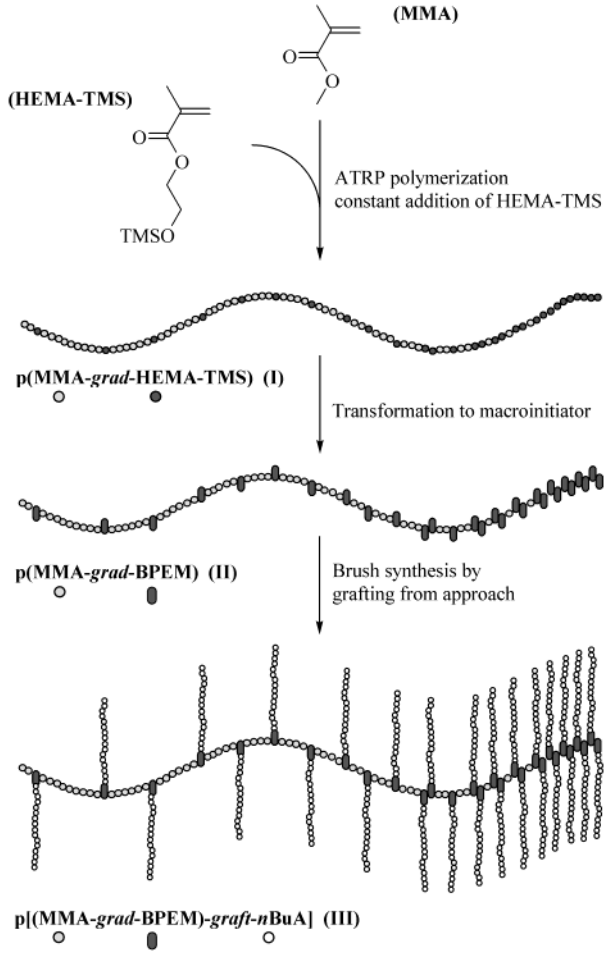

[†] Carnegie Mellon University.
[‡] University of North Carolina at Chapel Hill.

10.1021/ma012100a CCC: $22.00
Published on Web 03/21/2002

methacrylate (HEMA-TMS), followed by transformation of the precursor polymer into poly(2-(2-bromopropionyloxy)ethyl methacrylate) (pBPEM).[14,15]

It was also demonstrated that ATRP is an appropriate method to synthesize gradient copolymers showing a constant overall composition per molecule and a comparable gradual change of instantaneous composition along each polymer chain.[23−26,27] The synthesis requires a controlled/"living" polymerization technique such as ionic polymerization or controlled radical polymerization. These methods exhibit simultaneous initiation of individual growing polymer chains with negligible transfer or termination and simultaneous growth (or fast exchange of the active growing species) between all polymer chains. Controlled radical polymerization is perhaps the most suitable technique for the synthesis of gradient copolymers. This is due to a facile cross-propagation for various monomers (acrylates/methacrylates, styrene/methacrylates, styrene/acrylonitrile) that cannot be achieved by ionic polymerization methods. Further advantages are the controllable polymerization rate and a low sensitivity to moisture and other protic impurities.

Gradient copolymers can be prepared either as spontaneous or forced gradients. In the former case copolymerization of monomers with different reactivity ratios (e.g., acrylates/methacrylates[27,28] or styrene/*n*-butyl acrylate[29]) leads to a continuous change in monomer composition of reaction mixture which results in a continuous change of composition along each individual polymer chain. In the latter case comonomers with similar reactivity can be used but a change of composition in the reaction mixture is accomplished by continuous addition of one comonomer (e.g., two methacrylate derivatives or styrene/acrylonitrile[30]).

In the present publication we report the synthesis of a macroinitiator exhibiting a continuous gradient of initiating group density along the polymer chain. This was achieved by applying ATRP in combination with gradient copolymerization techniques. The gradient macroinitiator was prepared by continuous addition of HEMA-TMS to ATRP of MMA; TMS groups were subsequently transformed to 2-bromopropionate groups and used to synthesize macromolecular brushes by grafting *n*-butyl acrylate (*n*BuA) from each initiation site under ATRP conditions (Scheme 1).

Experimental Section

Starting Materials. Copper(I) bromide (Aldrich, 98%) was purified as described previously. Copper(II) bromide (Aldrich, 99+%) was used as received. To increase accuracy of $CuBr_2$ addition, a $CuBr_2$/(dNbpy)$_2$ stock solution in butanone was used (0.609 g of $CuBr_2$ per 100 g of solution) (the addition was based on weight). Tosyl chloride (TosCl) was recrystallized from hexane. 4,4′-Di-(5-nonyl)-2,2′-bipyridyl (dNbpy) was prepared as described previously.[31] 2-Bromopropionyl bromide was distilled under vacuum (10^{-1} mbar) at 45 °C prior to use. Tetrahydrofuran (THF) was distilled from sodium/benzophenone prior to use. Methyl methacrylate was distilled over calcium hydride and stored at −15 °C. Synthesis of HEMA-TMS[32] was carried out according to procedures in the literature. All other reagents and solvents were used as received from Aldrich or ACROS Chemicals.

Measurements. Monomer conversion was determined using a Shimadzu GC 17A gas chromatograph equipped with a AO20ic autosampler and a FID detector using a J&W Scientific 30 m DB608 column. Injector and detector temperatures were kept constant at 250 °C (conditions for GC analysis: anisole, xylene (internal standards)/HEMA-TMS, MMA (monomers): start temperature 40 °C, isotherm 3 min, heating rate 20 °C/min, final temperature 160 °C, isotherm 0 min). A linear response of the FID detector for all components in the used concentration range was observed. The conversion was calculated by detecting the decrease of the monomer peak area relative to the standard peak area. The HEMA-TMS addition was calculated by detecting the increase of the anisole peak area relative to the xylene peak area. GC measurements were repeated three times for each sample to reduce errors.

The molecular weight was determined by gel permeation chromatography (GPC) equipped with Waters microstyragel columns (pore size 10^5, 10^4, 10^3 Å), a differential refractometer (Waters model 410), and PSS GPC Win software. Measurements were conducted in THF (35 °C), at a flow rate of 1 mL/min. The setup was calibrated against low-polydispersity poly(methyl methacrylate) (pMMA) standards (PSS, Germany) with toluene as internal standard.

^{1}H NMR characterization was performed on a Bruker 300 MHz spectrometer. The measurements were carried out in chloroform-*d*. The overall ratio of incorporated monomer in MMA/BPEM copolymer was determined using ^{1}H NMR measurements by comparing the peak area ratio of characteristic signals for pMMA ($\delta = 3.6$ ppm, 3H, s, $-O-CH_3$) to pBPEM ($\delta = 4.52$ ppm, 1H, q, $J = 6.8$ Hz, $Br-CH-CH_3$; $\delta = 4.36$ ppm, 2H, bs, $-O-CH_2-CH_2-O-CO-CH-Br$). The side chain length in p*n*BuA brushes was determined by comparison of peak area ratio of characteristic signals for the macroinitiator ($\delta = 3.6$ ppm, s, 3H, $-O-CH_3$ characteristic for pMMA part of macroinitiator to p*n*BuA ($\delta = 4.0$ ppm, bs, 3H, $-O-CH_2-CH_2-CH_2-CH_3$).

Conversion of graft polymerization was determined by monomer consumption based on gravimetry. The side chain degree of polymerization was calculated on the basis of conversion assuming quantitative initiation from each Br atom, $DP_{conv} = \Delta[M]/[I]_0$, and ^{1}H NMR as described above.

Atomic force micrographs were recorded with a Nanoscope IIIa instrument (Digital Instruments) operating in the tapping mode. The measurements were performed at ambient conditions (in air, 56% relative humidity, 27 °C) using Si cantilevers with a spring constant of ca. 50 N/m, a tip radius of 8 nm, and a resonance frequency of about 300 kHz. The set-point amplitude ratio was varied in a broad range from 0.4 to 0.9 to attain clear resolution of the side chains. While the side chains were resolved at lower ratios, height profiles of adsorbed molecules were measured at higher values of the amplitude ratio to minimize tip indentation. The samples for tapping mode SFM measurements were prepared by spin-casting at 2000 rpm of dilute solutions of brush molecules in chloroform.

Synthesis of pMMA (Test Reaction). Copper(II) bromide (0.0017 g, 0.0075 mmol, 0.278 g stock solution) and dNbpy (0.115 g, 0.28 mmol) were dissolved in MMA (10 g, 10.6 mL, 99.80 mmol) in a 50 mL Schlenk flask. The mixture was degassed by three freeze/pump/thaw cycles and stirred for 30 min. In a separate round-bottom flask, tosyl chloride (TosCl, 0.038 g, 0.20 mmol) was dissolved in 3.54 mL of xylene (25 vol %). The mixture was cooled to 0 °C and degassed by bubbling with nitrogen gas for 20 min. Copper(I) bromide (0.022 g, 0.15 mmol) was added to the Schlenk flask, stirred for 15 min at room temperature (rt) to allow copper−ligand complex formation, and placed in a preheated oil bath at 90 °C. The initiator solution was cannula transferred into the Schlenk flask. The solution turned from dark red to green and back to red again within 1 min. Samples were taken to determine conversion by GC and molecular weight by GPC. After 5 h, the flask was cooled to rt and exposed to air: 59.4% conversion (GC); $M_{n,th} = 30\,100$ (assuming complete initiation); M_n(GPC) = 26 300; $M_w/M_n = 1.23$. Initiator efficiency was calculated on the basis of linear regressions of the number-average weight vs reaction time plots ($In_{eff} = M_{n,th}/M_n$(GPC) = 87.4%).

Synthesis of p(MMA-*grad*-HEMA-TMS). In the primary reaction Schlenk flask $CuBr_2$ (0.0010 g, 0.0046 mmol, 0.173 g stock solution), dNbpy (0.075 g, 0.18 mmol), and MMA (3.10 g, 3.3 mL, 30.98 mmol) were combined, and the mixture was degassed three times by freeze/pump/thaw cycles. In the

secondary reaction Schlenk flask $CuBr_2$ (0.0011 g, 0.0051 mmol, 0.190 g stock solution), dNbpy (0.083 g, 0.20 mmol), 2.55 mL of anisole, and HEMA-TMS (6.90 g, 7.1 mL, 34.08 mmol) were added and degassed by three freeze/pump/thaw cycles. CuBr (0.013 g, 0.09 mmol) was added to the primary and also (0.015 g, 0.10 mmol) to the secondary mixture. After stirring the mixtures for 30 min, initial samples (GC) were taken from both the primary and secondary mixtures. The secondary reaction mixture was transferred into an airtight syringe and assembled to a syringe pump. An initiation solution was prepared by dissolving TosCl (0.024 g, 0.12 mmol) in 1.07 mL of xylene followed by degassing by bubbling with N_2 for 10 min at 0 °C. The primary flask was placed in a preheated oil bath at 90 °C, and the initiation solution was added. Simultaneously, the continuous addition of the secondary reaction mixture to the primary one was started at a rate of 1.52 mL/h. Samples were taken of about 0.1−0.2 mL every 30 min. After 6.3 h, the HEMA-TMS addition was complete. The reaction was stopped after 7 h by cooling the flask to rt and exposing the reaction mixture to air. Monomer conversion was found to be 66% MMA and 31% HEMA-TMS (GC); $M_{n,th}$ = 44 100; M_n(GPC) = 56 700; M_w/M_n = 1.22.

The polymer solution was diluted with $CHCl_3$ and passed over an alumina column to remove the catalyst. The solvent was distilled off under vacuum using a rotary evaporator at 25 °C, and the polymer was dried under vacuum (10^{-2} mbar) for 24 h.

Synthesis of p(MMA-*grad*-BPEM). The product of the p(MMA-*grad*-HEMA-TMS) polymerization was placed in a 250 mL round-bottom flask (assuming 10.40 mmol of R−OTMS groups). After KF (0.604 g, 10.40 mmol) addition, the flask was sealed and flushed with N_2, and 125 mL of dry THF was added. Tetrabutylammonium fluoride (0.027 g, 0.03 mL, 0.10 mmol) was added dropwise to the flask, followed by the slow addition of 2-bromopropionyl bromide (3.37 g, 1.65 mL, 15.6 mmol) over the course of 15 min. The reaction mixture was stirred at room temperature for 4 h and afterward precipitated into methanol/ice (80/20 v/v %). The separated precipitate was redissolved in 200 mL of $CHCl_3$ and filtered through a column of activated alumina (basic), and the solvent was removed in a vacuum. The isolated polymer was reprecipitated from THF once in MeOH, three times in hexanes, and dried under vacuum at 25 °C for 24 h. 2.3 g of p(MMA-*grad*-BPEM) was obtained (43% yield). Complete conversion was determined by ^{1}H NMR (absence of TMS−O− resonance (δ = 0.2 ppm (9H, bs, ($H_3C)_3Si$−))). M_n(GPC) = 53 200; M_w/M_n = 1.12. ^{1}H NMR (300 MHz, $CDCl_3$, δ in ppm): pBPEM part: 4.52 (1H, quart., J = 6.8 Hz, Br−C*H*-CH_3); 4.36 (2H, bs, −O−CH_2−CH_2−O−CO−CH−Br); 4.15 (2H, bs, −O−CH_2−CH_2−O−CO−CH−Br); 1.82 (overlapped, d, J = 6.8 Hz, Br−CH−CH_3); 2.21−1.44 (overlapped, m, CH_2−C−CH_3); 1.22−0.94 (overlapped, 3 × bs, CH_2−C−CH_3). pMMA part: 3.6 (3H, s, −O−CH_3); 2.15−1.37 (overlapped, m, CH_3−C−CH_2); 1.37−0.75 (overlapped, 3 × bs, CH_3−C−CH_2). Overall ratio [MMA]:[BPEM] (^{1}H NMR) = 71:29; [MMA]:[BPEM] (elemental analysis) = 68:32.

p[(MMA-*grad*-BPEM)-*graft*-*n*BuA]. In a 100 mL Schlenk flask p(MMA-*grad*-BPEM) (0.2 g; 0.550 mmol initiating sites (based on GC conversion)), $CuBr_2$ (0.0028 g, 0.0126 mmol, 0.469 g stock solution), and dNbpy (0.206 g, 0.51 mmol) were purged three times with inert gas. Deoxygenated *n*BuA (25.92 g, 28.9 mL, 0.202 mol) and butanone (9.6 mL, 25 v%) were added, and the reaction mixture was degassed by three freeze/pump/thaw cycles. After stirring for 1 h at rt, CuBr (0.0363 g, 0.253 mmol) was added, and the flask was placed in a preheated oil bath at 70 °C. The polymerization was stopped after 24 h by cooling to rt and opening the flask to air. GPC was used to analyze the molecular weight and the polydispersity ($M_{n,app}$ = 359 500 and M_w/M_n = 1.26).

The polymer was purified by distilling off both the solvent and the monomer under vacuum (2 × 10^{-2} mbar) at room temperature, dissolving the crude polymer in chloroform (about 100 mL), and passing it through a column (2 cm × 13 cm) of alumina, followed by removing the solvent on a rotary evaporator (25 °C) and drying the product in high vacuum at room temperature for 24 h. Yield: 2.79 g isolated polymer ($DP_{sc,grav}$ = 40). ^{1}H NMR (300 MHz, $CDCl_3$, proton resonances used for integration were given in the method section): p*n*BuA:pMMA = 7.9:1; DP_{sc}(NMR) = 34.

Using the same procedure, p[(MMA-*grad*-BPEM)-*graft*-*n*BuA] was prepared by grafting *n*BuA from p(MMA-*grad*-BPEM). Reaction conditions: $[M]_0$:$[In]_0$:$[CuBr]_0$:$[CuBr_2]_0$:$[dNbpy]_0$:$[MEK]_0$ = 400:1:0.5:0.025:1:25 vol %; 70 °C; 6 h; $M_{n,app.}$ = 138 900 and M_w/M_n = 1.12 (GPC); $DP_{sc,grav}$ = 15. ^{1}H NMR (300 MHz, $CDCl_3$): p*n*BuA:pMMA = 16.7:1; DP_{sc}(NMR) = 16.

Results and Discussion

Copper-mediated atom transfer radical polymerization and the "forced gradient" technique was applied to the synthesis of poly(MMA-*grad*-HEMA-TMS). This semibatch method involves the continuous addition of HEMA-TMS to a MMA polymerization. In contrast to spontaneous gradient copolymerization, where different reactivity ratios of two simultaneously copolymerized monomers lead to formation of the gradient structure, the gradient composition can be varied by monomer addition over a broader range using "forced gradient" technique. Two methacrylate derivatives were chosen in order to ensure efficient cross-propagation (e.g., of reactivity ratios of MMA ($r_{1,2}$)/MA derivatives ($r_{2,1}$) (MMA (1.08)/EtMA (1.08), MMA (1.21)/PrMA (1.24);[33] MMA (0.93)/BenzMA (1.05);[34] MMA (0.96)/*t*BuMA (1.35),[35] MMA (0.98)/*n*BuMA (1.26)[36]). However, the continuous monomer addition that allows the flexibility of this approach causes some difficulties by a continuous change of the catalyst and initiator concentration. Furthermore, characterization of the evolution of molecular weight, polydispersity, and polymer composition during polymerization is not possible without changing some polymerization parameters, since taking a sample changes the feed ratio. Therefore, the minimal sample sizes were used to reduce these variations.

The first method to confirm the formation of a gradient copolymer was monitoring the copolymer composition by ^{1}H NMR. Therefore, a sample has to be taken large enough to remove monomer from the polymer (0.4−0.5 mL). Since HEMA-TMS has a high boiling point, a precipitation method has be applied which, especially in the early stage of polymerization, could lead to fractionation, making composition data less reliable. The second method was to monitor the comonomer consumption, assuming complete conversion of consumed monomer to polymer. This method requires smaller samples (0.1−0.2 mL). Online spectroscopy methods might be another possibility to analyze the system without disruption.

Gradient Copolymer Synthesis. Since a continuous gradient from 100% pMMA on one side of the polymer chain to 90% pHEMA-TMS on the other side was targeted, the addition rate of the second monomer (HEMA-TMS) had to be synchronized with the polymerization rate. Therefore, test reactions were necessary to determine the polymerization rate of MMA using reaction conditions comparable to the conditions used in the gradient copolymerization (Table 1).

As shown in Figure 1, monomer conversion in the MMA polymerization under ATRP conditions proceeds linearly with time. After 5 h the reaction was stopped at 61% monomer conversion. The resulting polymer had a M_n = 26 300 and a polydispersity of M_w/M_n = 1.2. By comparison of the theoretical number-average molecular weight calculated on the basis of monomer conversion, with the experimental values determined by GPC

Table 1. Reaction Conditions for MMA Test Reaction and Gradient Synthesis[a]

reaction		$[monomer]_0$	$[TosCl]_0$	$[solvent]_0$
homopolymerization (pMMA)	*b*	500 MMA	1	25 vol % (xylene)
gradient copolymerization	primary mixture[b]	250 MMA	1	25 vol % (xylene)
(p(MMA-*grad*-HEMA-TMS))	secondary mixture[c]	275 HEMA-TMS		25vol % (anisole)

[a] Reaction temperature: 90 °C. [b] $[CuBr]_0:[CuBr_2]_0:[dNbpy]_0 = 0.75:0.0375:1.575$. [c] $[CuBr]_0:[CuBr_2]_0:[dNbpy]_0 = 0.82:0.0412:1.732$.

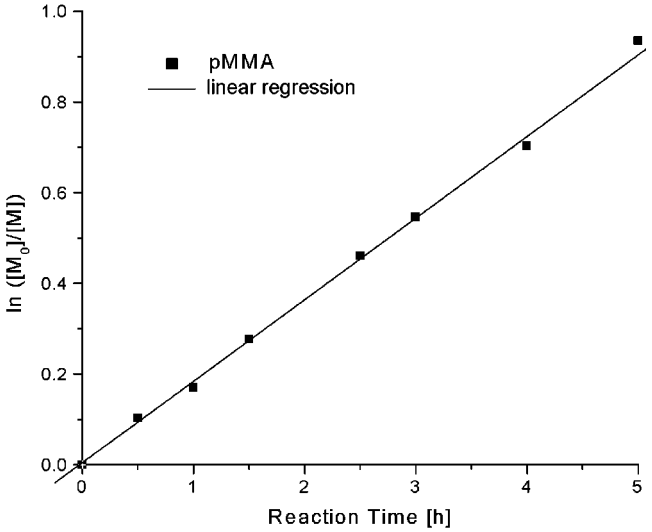

Figure 1. Monomer conversion of the MMA test reaction.

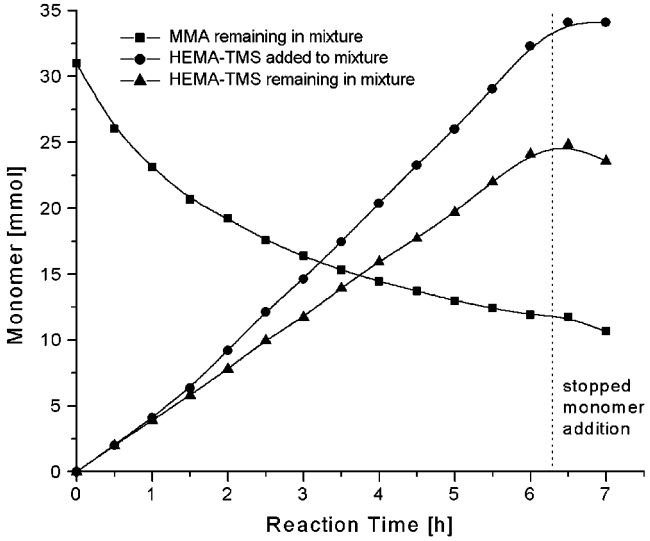

Figure 2. Evolution of monomer concentration during gradient copolymerization.

calibrated against pMMA standards, an initiation efficiency was calculated (In_{eff} = 80%). In a case of gradient copolymer synthesis 75% monomer conversion was targeted. Because of vitrification of the MMA test polymerization mixture, 75% conversion could not be reached. Therefore, this point was obtained by extrapolation from the presented data ($t_{75\%} \approx 6.3$ h).

The reaction conditions of the MMA test reactions (Table 1) were taken as a starting point to adapt the batch process to the semibatch gradient copolymerization. The following approach was chosen to synthesize poly(MMA-*gradient*-HEMA-TMS) (p(MMA-*grad*-HEMA-TMS)): A primary polymerization of MMA was performed under ATRP conditions (Table 1). Through constant addition of HEMA-TMS to the primary polymerization using a syringe pump (1.52 mL/h), the feed ratio was continuously shifted from 100% MMA in the beginning to 69% HEMA-TMS at the end of the polymerization. The optimized polymerization conditions are given in Table 1. In comparison to the MMA test reaction, one-half of the MMA monomer was removed from the primary polymerization mixture and substituted by HEMA-TMS, which was placed as a secondary reaction mixture in the motor syringe pump. Two different solvents were used (MMA/xylene; HEMA-TMS/anisole), providing the possibility to follow the feed ratio of the polymerization mixture and the monomer conversion of both monomers by GC analysis. To reach high incorporation of HEMA-TMS at the end of the copolymerization, the feed ratio of HEMA-TMS was enlarged by 10%. To avoid a significant decrease in polymerization rate, catalyst was added along with the second comonomer. This avoids dilution of the catalyst. Despite this, the initiator was continuously diluted, resulting in a decrease in polymerization rate. This made prediction of polymerization rate under these conditions difficult.

Figure 2 shows the variation of the relative concentrations of both monomers during the polymerization. This kinetic data were obtained by measuring monomers by GC relative to internal standards (anisole, xylene). Fast consumption of MMA can be observed during the early stage of the polymerization as a result of a high initiator concentration and a low concentration of competing HEMA-TMS. During the polymerization the rate of consumption of MMA slowed down due to a dilution of MMA with increasing amount of HEMA-TMS. After finishing the addition of HEMA-TMS (6.3 h) 62% of MMA has been converted to polymer. The rate of consumption of HEMA-TMS increases during the polymerization, due to the higher molar ratio in the feed. After 6.3 h 26% of HEMA-TMS was consumed. The polymerization was allowed to proceed for an additional 0.7 h, resulting in a small statistical copolymer block at the end of the gradient copolymer. After the monomer addition was stopped, polymerization still proceeded, which was indicated by a decrease of the amount of both MMA and HEMA-TMS.

On the basis of the monomer conversion data, and 87% initiation efficiency as determined from the MMA test polymerization, the theoretical number-average molecular weight was calculated. An increased initiator concentration in comparison to the MMA test polymerization might lead to a higher initial termination rate of initiator radicals. Since tosyl chloride was used, the recombination of tosyl radicals is reversible and should not affect initiation efficiency.[37] In Figure 3 the theoretical molecular weights are compared to the experimental values determined by GPC calibrated against pMMA standards. Up to 3 h, M_n(GPC) correlates well with $M_{n,conv}$(GC). This is due to the high amount of MMA incorporated in the polymer. At these ratios the incorporated HEMA-TMS shows no obvious effect on the hydrodynamic volume−molecular weight dependence, which is the critical relationship in gel permeation chromatography. After 3 h, deviation between M_n(GPC) and $M_{n,conv}$(GC) can be observed. This is reasonable since

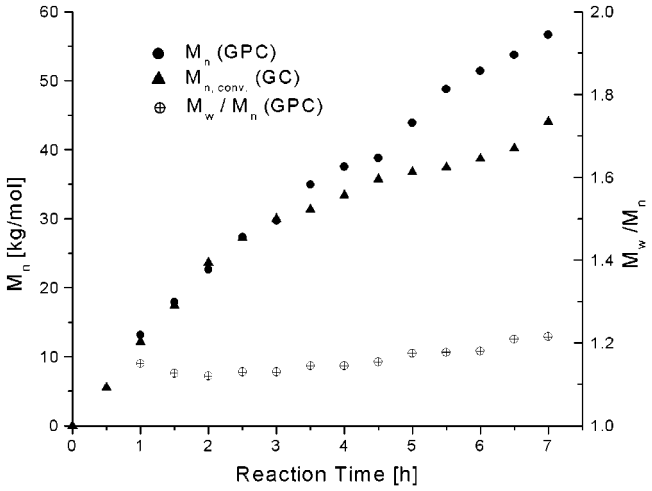

Figure 3. Evolution of molecular weights during gradient copolymerization.

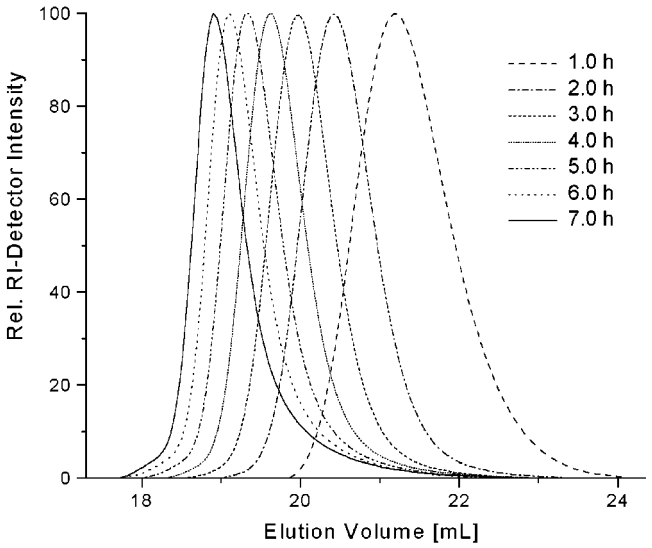

Figure 4. GPC traces of the syntheses of poly(MMA-*grad*-HEMA-TMS).

the decrease of the overall MMA to HEMA-TMS ratio in the formed copolymer results in an increasingly different behavior of the copolymer in comparison to narrow pMMA standards.

GPC traces of samples taken at hourly intervals are presented in Figure 4. It can be observed that the curves shift smoothly toward higher molecular weight. There is no significant broadening or tailing visible, indicating a controlled polymerization reaction. This is supported by the fact that the polydispersity remains at a constant value of about $M_w/M_n = 1.2$ during the entire polymerization. This relatively low value shows the advantage of choosing MMA as the primary polymerized monomer rather than HEMA-TMS. When HEMA-TMS had been used as the primary polymerized monomer, the polydispersity were around $M_w/M_n = 1.3$. This is consistent with the observation that the homopolymerization of HEMA-TMS is more difficult to control than MMA.[38]

In living or controlled polymerizations examination of the semilogarithmic conversion plot vs time is normally used to demonstrate the living character of the polymerization.[39−41] However, since monomer conversion in the described gradient copolymerization system depends on the monomer addition rate (e.g., if monomer addition is faster than monomer consumption, it will result in decreasing conversion), another plot has to be chosen to demonstrate the living character of this system.

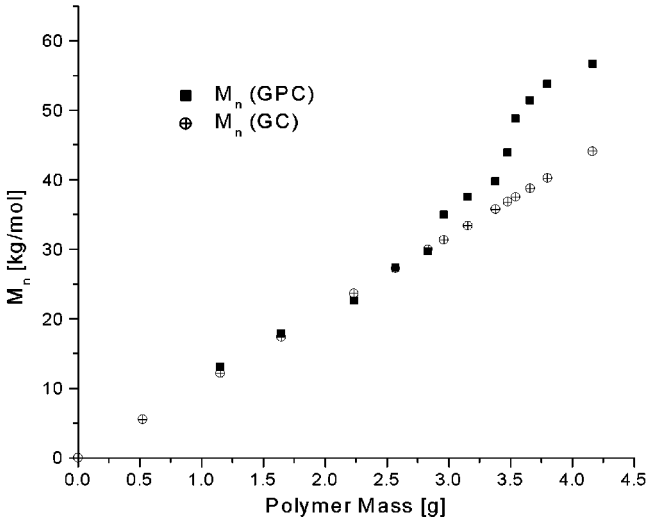

Figure 5. Molecular weights vs polymer yield based on monomer conversion of the poly(MMA-*grad*-HEMA-TMS) synthesis.

In Figure 5 the number-average molecular weight ($M_{n,conv}$(GC), M_n(GPC)) is plotted vs the overall mass of obtained polymer. A linear dependence between the experimental M_n determined by GPC and the weight of produced polymer indicates a constant number of growing chains. Since the calculation for $M_{n,conv}$(GC) assumes a constant number of chains, these values can be considered as the theoretical ones. Figure 5 shows a good agreement up to 30 000 g/mol between the experimental (M_n(GPC)) and the theoretical ($M_{n,conv}$(GC)) values, which indicates a constant number of chains. At molecular weights higher than 30 000 g/mol increasing deviation was observed. This could be due to termination reactions either by chain−chain coupling or by radical disproportionation followed by incorporation of the unsaturated species into the polymer. However, low polydispersity is maintained throughout the reaction (Figure 3) and suggests that a controlled polymerization occurred under these conditions. Therefore, it is more likely that increased incorporation of HEMA-TMS into the gradient copolymer results in the increased deviation in molecular weight predicted on the basis of linear pMMA standards.

The increase in degree of polymerization and the change in instantaneous composition can be accessed using monomer conversion data determined by GC. In Figure 6 the instantaneous proportion of composition along an average copolymer chain is presented. The average, instantaneous composition in each segment decreases continuously from 100% MMA in the beginning of the average polymer chain to around 12% at the end. These data confirm the synthesis of a gradient structure. The overall composition was pMMA:pHEMA-TMS = 66:34 (mol %) (Table 2).

From the literature it is known that derivatives of methacrylic esters have comparable reactivity ratios.[33−36] Simultaneous copolymerizations, using a broad range of monomer feed ratios of MMA and HEMA-TMS,[38] indicated comparable reactivity ratios, since the monomer feed was well reflected in the polymer composition.

Based on the instantaneous segment composition and the monomer feed ratios, a copolymerization diagram

Table 2. Analysis of Macroinitiator Precursor, Macroinitiator, and Macromolecular Brushes

reaction	$M_{n,app}$ [c]	M_w/M_n [c]	composition [mol %]
p(MMA-*grad*-HEMA-TMS)	53 000	1.21	67:33 (GC)[a]
p(MMA-*grad*-BPEM)	53 200	1.12	68:32 (elem analy);[b] 71:29 (NMR)[b]
p(MMA-*grad*-BPEM)-*graft*-*n*BuA(i)	202 600	1.12	DP_{SC} = 16 (NMR) DP_{SC} = 15 (grav)
p(MMA-*grad*-BPEM)-*graft*-*n*BuA(ii)	403 000	1.19	DP_{SC} = 33 (NMR) DP_{SC} = 40 (grav)

[a] [MMA]:[HEMA-TMS]. [b] [MMA]:[BPEM]. [c] GPC(THF, RI detector, pMMA standards).

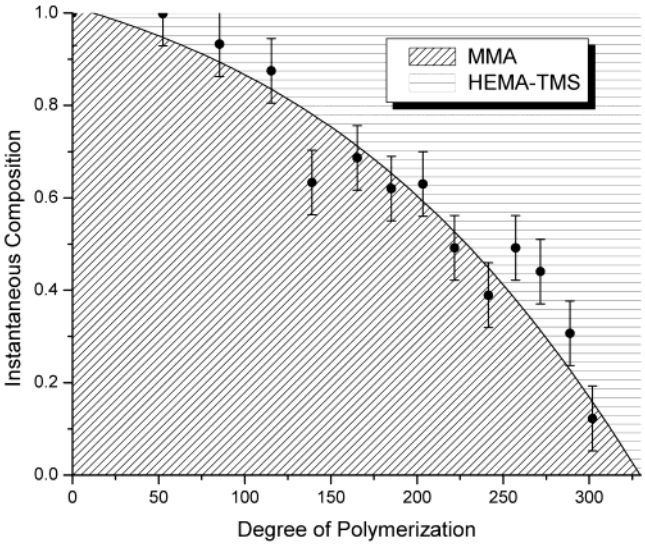

Figure 6. Instantaneous composition of poly(MMA-*grad*-HEMA-TMS).

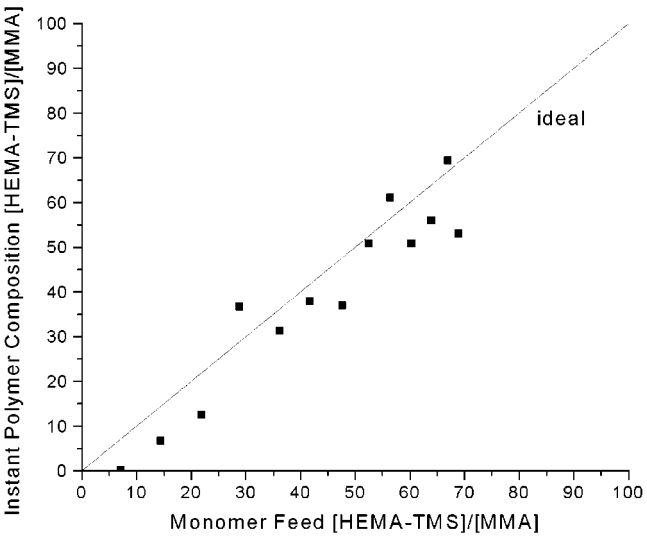

Figure 7. Copolymerization diagram (MMA/HEMA-TMS) based on instantaneous polymer and reaction mixture composition during synthesis of poly(MMA-*grad*-HEMA-TMS).

can be presented (Figure 7). Within the experimental error of this method, the instantaneous polymer composition reflects the monomer feed ratio in the range of the experimental values.

Transformation of pMMA-*grad*-HEMA-TMS into the Macroinitiator. The synthesized gradient copolymer (pMMA-*grad*-HEMA-TMS) was transformed to the macroinitiator (pMMA-*grad*-BPEM). The product was characterized by GPC against pMMA standards (Table 2). Figure 8 presents the overlaid GPC traces of the starting material and isolated product. The macroinitiator trace is shifted entirely to higher molecular weight. No significant shoulder can be observed, indicating negligible contributions of side reactions. Molecular weight was determined to be M_n = 53 200, and the polydispersity remains narrow (M_w/M_n = 1.12). Complete transformation can be confirmed by ^{1}H NMR (absence of characteristic Me_3Si- proton resonance) as well as by elemental analysis. Furthermore, both analytical methods verify the overall comonomer ratio found by each monomer conversion (GC) of pMMA:pBPEM = 66:34 (by ^{1}H NMR pMMA:pBPEM = 71 ± 5:29 ± 5; by elemental analysis pMMA:pBPEM = 68:32). For a polymer with the molecular weight M_n = 53 200, the ratio 66:34 gives the number-average degree of polymerization N_n = 341, assuming that M_{MMA} = 100 and M_{BPEM} = 265 are molecular weights of MMA and BPEM, respectively.

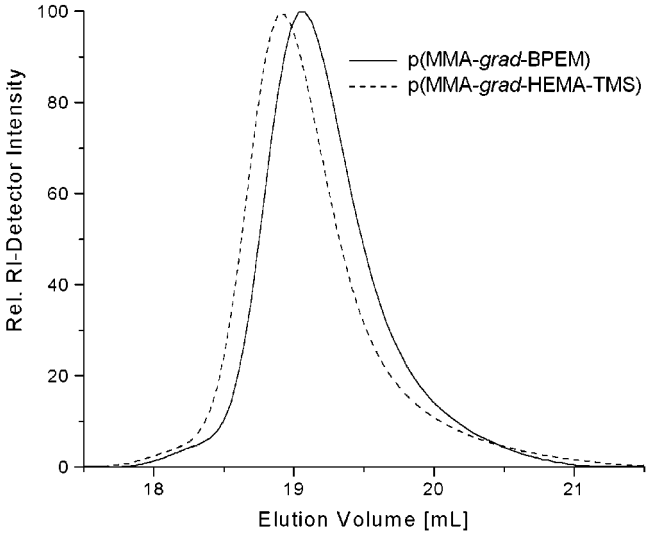

Figure 8. GPC traces of the synthesis of poly(MMA-*grad*-BPEM) macroinitiator.

Synthesis of Graft Copolymers. Two graft copolymers with different side chain lengths were synthesized by grafting *n*BuA from the p(MMA-*grad*-BPEM) macroinitiator (Table 2). As shown in Figure 9, the GPC traces shift completely to higher molecular weight; no shoulder formation can be observed, giving no evidence for brush−brush coupling reactions. The apparent molecular weights (based on PSt standards) increase toward $M_{n,app}$ = 202 600 for p[(MMA-*grad*-BPEM)-*graft*-*n*BuA(i)] and $M_{n,app}$ = 403 000 for p[(MMA-*grad*-BPEM)-*graft*-*n*BuA(ii)]. Since the polydispersity remains relatively narrow (p[(MMA-*grad*-BPEM)-*graft*-*n*BuA(i)] M_w/M_n = 1.12 and p[(MMA-*grad*-BPEM)-*graft*-*n*BuA(ii)] M_w/M_n = 1.19), the polymerization reaction appears in a controlled manner. The average degree of polymerization of pnBuA side chain polymer was analyzed by gravimetry and NMR (p[(MMA-*grad*-BPEM)-*graft*-*n*BuA-(15)]: $DP_{sc,grav}$ = 15, $DP_{sc,NMR}$ = 16; p[(MMA-*grad*-BPEM)-*graft*-*n*BuA(ii)]: $DP_{sc,grav}$ = 40, $DP_{sc,NMR}$ = 33). In all cases the determined side chain lengths agree within the experimental error.

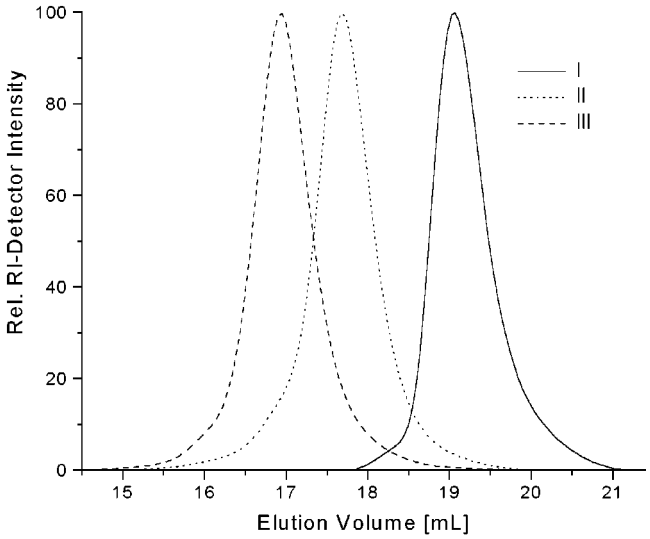

Figure 9. GPC traces of the subsequent molecular brush synthesis of (I) poly(MMA-*grad*-BPEM) and (II) poly[(MMA-*grad*-BPEM)-*graft*-*n*BuA(i)]; poly[(MMA-*grad*-BPEM)-*graft*-*n*BuA(ii)].

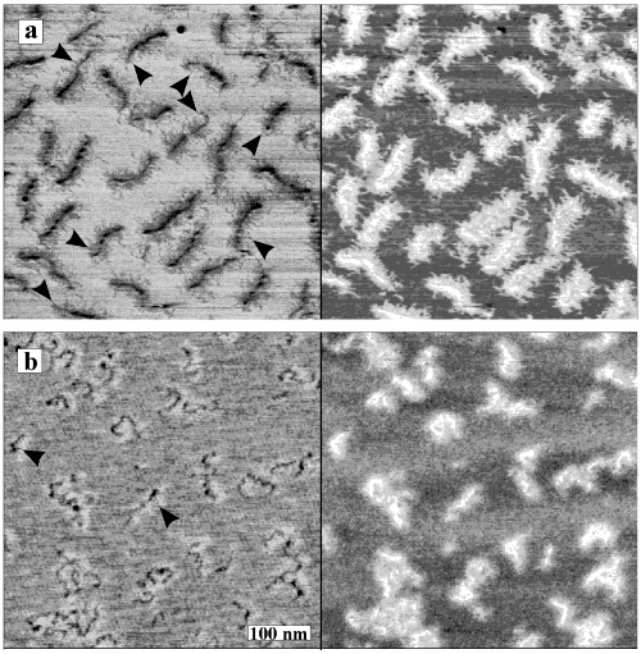

Figure 10. Tapping mode AFM was used to measure height and phase micrographs of gradient brushes with a degree of polymerization of the side chains: (a) $n = 40$ and (b) $n = 15$. The height micrographs (left side) are presented as inverted to enhance the image contrast. The phase micrographs (right side) reveal a corona of side chains around the backbone due to the strong mechanical contrast relative to the underlying mica. However, the phase images demonstrate less contrast between the side chains and the backbone.

AFM Analysis of Gradient Copolymers. Visualization of individual molecules by atomic force microscopy provided additional evidence for the gradient structure. The particular strength of this method in application to brush macromolecules is due to its ability to resolve for individual molecules the fine molecular structure including the backbone and the side chains.[22] Figure 10 shows height micrographs of two brush molecules with different length of the side chains ($n = 40$ and $n = 15$). The hairy structure of the side chains was clearly visualized for both types of brushes. A better contrast was achieved for brushes with longer side chains, i.e., $n = 40$. Brush molecules in Figure 10a are more extended and show larger lateral dimensions (height and width). Both the height and the phase micrographs in Figure 10a revealed an uneven distribution of the side chains along the backbone. The molecules demonstrate a bulky head and a thin tail. The most characteristic molecules are indicated by arrows in Figure 10. The head part of the molecules is surrounded by a dense shell of the side chains. In contrast, the tail part contains a fewer number of the side chains and results in a fuzzy structure in the AFM micrographs.

Since both types of the brush molecules were grown from the same backbone, one can measure its apparent length from the AFM images and compare it to the length of a fully extended main chain. The latter can be estimated from the GPC data as $L_0 = N_n l_0$, where $N_n = 341$ is the number-average degree of polymerization of the macroinitiator, i.e., backbone, and $l_0 \cong 0.25$ nm is the monomer length of a carbon chain assuming the all-trans conformation. Therefore, a completely extended chain with a degree of polymerization $N = 341 \pm 20$ would give $L_0 = 85 \pm 5$ nm. Contour-length measurements from AFM images were fairly accurate for brushes with longer side chains, which demonstrate extended conformation (Figure 10a). The number-average and the length average molecular lengths were determined to be 87 ± 4 nm and 91 ± 4 nm, respectively. The fact that the number-average length $L_n = 87$ is very close to $L_0 = 85$ nm indicates nearly complete extension of the main chain. Previously, the extension has been shown to be caused by steric repulsion of the adsorbed side chains.[22] The polydispersity index for the chain length, $L_w/L_n = 1.05$, is consistent with the molecular weight polydispersity $M_w/M_n = 1.12$ determined by GPC. AFM images of brushes with shorter side chains were more difficult to analyze due to their coiled conformation. The pronounced flexibility interferes in visualization of the backbone and decreases accuracy of the length measurements in Figure 10b. The average lengths was determined as $L_n = 71 \pm 9$ nm and $L_w = 78 \pm 9$ nm. Therefore, the short-side-chain brushes contracted axially compared to the brushes with longer side chains.

Conclusion

A well-defined macroinitiator was synthesized by gradient copolymerization of MMA with HEMA-TMS, followed by transformation of the precursor poly(MMA-*gradient*-HEMA-TMS) into poly(MMA-*gradient*-BPEM). The macroinitiator exhibits a gradient in spacing between the ATRP initiation groups ranging from 0 mol % initiation sites on one end to 90 mol % on the other. From this macroinitiator *n*-butyl acrylate was grafted under ATRP conditions. This leads to well-defined macromolecular brushes with *n*-butyl acrylate side chains and methacrylate backbone showing a gradient in spacing between the side chains along the backbone. AFM measurements visualize the resulting asymmetric brushes with a bulky head and a thinner tail.

Acknowledgment. This work was financially supported by the National Science Foundation (ECS-01 03307) and a Humboldt Research Award for US Senior Scientists for K.M. We acknowledged many fruitful discussions with Prof. Martin Moeller.

References and Notes

(1) Sheiko, S.; Moeller, M. *Chem. Rev.* **2001**, *101*, 4099.
(2) Tsukahara, Y.; Tsutsumi, K.; Yamashita, Y.; Shimada, S. *Macromolecules* **1990**, *23*, 5201.
(3) Subbotin, A.; Saariaho, M.; Ikkala, O.; ten Brinke, G. *Macromolecules* **2000**, *33*, 3447.
(4) Ruokolainen, J.; Saariaho, M.; Ikkala, O.; ten Brinke, G.; Thomas, E. L.; Torkkeli, M.; Serimaa, R. *Macromolecules* **1999**, *32*, 1152.
(5) Hsieh, H. L.; Quirk, R. P. *Anionic Polymerization. Principle and Practical Applications*; Marcel Dekker: New York, 1996.
(6) Fredrickson, G. H. *Macromolecules* **1993**, *26*, 2825.
(7) Schappacher, M.; Deffieux, A. *Macromolecules* **2000**, *33*, 7371.
(8) Yamada, K.; Miyazaki, M.; Ohno, K.; Fukuda, T.; Minoda, M. *Macromolecules* **1999**, *32*, 290.
(9) Djalali, R.; Hugenberg, N.; Fischer, K.; Schmidt, M. *Macromol. Rapid Commun.* **1999**, *20*, 444.
(10) O'Donnell, P. M.; Brzezinska, K.; Wagener, K. B. *Polym. Prepr.* (*Am. Chem. Soc., Div. Polym. Chem.*) **1999**, *40*, 138.
(11) Wintermantel, M.; Gerle, M.; Fischer, K.; Schmidt, M.; Wataoka, I.; Urakawa, H.; Kajiwara, K.; Tsukahara, Y. *Macromolecules* **1996**, *29*, 978.
(12) Rempp, P.; Lutz, P.; Masson, P.; Chaumount, P.; Franta, E. *Macromol. Chem. Suppl.* **1985**, *13*, 47.
(13) Beers, K. L.; Gaynor, S. G.; Matyjaszewski, K.; Sheiko, S. S.; Prokhorova, S. A.; Moeller, M. *Polym. Prepr. (Am. Chem. Soc., Div. Polym. Chem.)* **1999**, *40* (2), 446.
(14) Beers, K. L.; Gaynor, S. G.; Matyjaszewski, K.; Sheiko, S. S.; Möller, M. *Macromolecules* **1998**, *31*, 9413.
(15) Boerner, H. G.; Beers, K. L.; Matyjaszewski, K.; Sheiko, S. S.; Moeller, M. *Macromolecules* **2001**, *34*, 4375.
(16) Wang, J. S.; M., K. *J. Am. Chem. Soc.* **1995**, *117*, 5614.
(17) Patten, T. E.; Matyjaszewski, K. *Acc. Chem. Res.* **1999**, *32*, 895.
(18) Patten, T. E.; Matyjaszewski, K. *Adv. Mater.* **1998**, *10*, 901.
(19) Matyjaszewski, K. *Chem. Eur. J.* **1999**, *5*, 3095.
(20) Matyjaszewski, K.; Xia, J. *Chem. Rev.* **2001**, *101*, 2921.
(21) Cheng, G.; Boeker, A.; Zhang, M.; Krausch, G.; Mueller, A. H. E. *Macromolecules* **2001**, *34*, 6883.
(22) Sheiko, S. S.; Prokhorova, S. A.; Beers, K. L.; Matyjaszewski, K.; Potemkin, I. I.; Khokhlov, A. R.; Moeller, M. *Macromolecules* **2001**, *34*, 8354.
(23) Wang, J.-S.; Greszta, D.; Matyjaszewski, K. *Polym. Mater. Sci. Eng.* **1995**, *73*, 416.
(24) Greszta, D.; Matyjaszewski, K. *Polym. Prepr. (Am. Chem. Soc., Div. Polym. Chem.)* **1996**, *37*, 569.
(25) Pakula, T.; Matyjaszewski, K. *Macromol. Theory Simul.* **1996**, *5*, 987.
(26) Matyjaszewski, K.; Ziegler, M. J.; Arehart, S. V.; Greszta, D.; Pakula, T. *J. Phys. Org. Chem.* **2000**, *13*, 775.
(27) Ziegler, M. J.; Matyjaszewski, K. *Macromolecules* **2001**, *34*, 415.
(28) Roos, S. G.; Mueller, A. H. G.; Matyjaszewski, K. *Macromolecules* **1999**, *32*, 8331.
(29) Arehart, S. V.; Matyjaszewski, K. *Macromolecules* **1999**, *32*, 2221.
(30) Greszta, D.; Matyjaszewski, K.; Pakula, T. *Polym. Prepr. (Am. Chem. Soc., Div. Polym. Chem.)* **1997**, *38*, 709−710.
(31) Matyjaszewski, K.; Patten, T.; Xia, J. *J. Am. Chem. Soc.* **1997**, *119*, 674.
(32) Beers, K. L.; Boo, S.; Gaynor, S. G.; Matyjaszewski, K. *Macromolecules* **1999**, *32*, 5772.
(33) Musha, Y.; Hori, Y.; Sato, Y.; Katayama, M. *Nihon Daigaku Kogakubu Kiyo, Bunrui A* **1985**, *26*, 175.
(34) Yuki, H.; Okamoto, Y.; Shimada, Y.; Ohta, K.; Hatada, K. *J. Polym. Sci., Polym. Chem. Ed.* **1979**, 1215.
(35) Bevington, J. C.; Malpass, B. W. *Eur. Polym. J.* **1965**, 1.
(36) Haddleton, D. M.; Crossman, M. C.; Hunt, K. H.; Topping, C.; Waterson, C.; Suddaby, K. G. *Macromolecules* **1997**, *30*, 3992.
(37) Percec, V.; Barboiu, B.; Kim, H. J. *J. Am. Chem. Soc.* **1998**, *120*, 305−316.
(38) Beers, K. L. Ph.D. Thesis, Carnegie Mellon University, Pittsburgh, PA, 2000.
(39) Penczek, S.; Kubisa, P.; Szymanski, R. *Makromol. Chem., Rapid Commun.* **1991**, *12*, 77−80.
(40) Quirk, R. P.; Lee, B. *Polym. Int.* **1992**, 359.
(41) Matyjaszewski, K. *J. Phys. Org. Chem.* **1995**, *8*, 197.

MA012100A